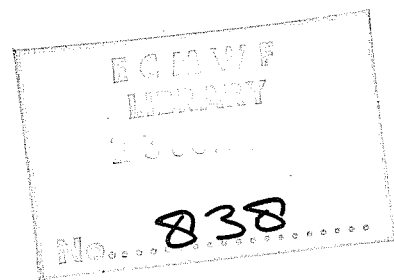


TECHNICAL REPORT No. 18

CONFIDENCE LIMITS FOR VERIFICATION AND ENERGETICS STUDIES

by

K. Arpe



May 1980

C O N T E N T S

PAGE

ABSTRACT	1
1. INTRODUCTION	1
2. DIFFERENCES BETWEEN ANALYSES	1
3. SENSITIVITY OF VERIFICATION AND DIAGNOSTIC PARAMETERS	9
4. CONCLUSIONS	20
REFERENCES	21
APPENDIX - DEFINITION OF SCORES	22

ABSTRACT

It is shown that the operational objective analyses by different meteorological centres demonstrate considerable deviations. They become even more obvious when the data are used for the calculation of derived quantities like kinetic and available potential energy or static stability. When comparing forecast results with the analyses for verification purposes, the choice of analyses schemes may be decisive for the conclusions. Some examples are given.

1. INTRODUCTION

Everyone looking at weather maps prepared by different analysts or different numerical methods would have detected differences even over data rich areas (e.g. Bliesner et al, 1977). The differences can mainly be found in the intensity of cyclones and anticyclones. Fig. 1 shows an example of 500 mb height fields analysed by the National Weather Services in the US (NMC), in Germany (DWD) and in the United Kingdom (UKM). In order to make the differences obvious, maps of differences are also shown. The largest values can be found over data sparse areas like the oceans and deserts. In the southern hemisphere the differences would probably be even greater. Over the Continents differences of 20 to 30 m are also quite common.

The aim of the present investigation is to find out whether such differences are important when using these analyses for verification or diagnostic purposes. It is not anticipated to find out which of the three analyses schemes is the best or the worst; only the range of uncertainty in the present knowledge of the atmospheric state will be shown.

In Section 2 we will see more about the differences in the analysis schemes for February 1976, and in Section 3 the sensitivity of a wide range of verification scores and diagnostic parameters to different sets of analysis data will be shown.

2. DIFFERENCES BETWEEN ANALYSES

Fig. 2 shows an average of 25 days (3 to 27 February 1976) of the 500 mb height field (panel a) made by DWD and the mean differences between DWD and NMC analyses for 12Z and 00Z analyses separately (panel b and c). As in the single case in Fig. 1 we find fairly big differences over the oceans and the Sahara where the NMC analyses have consistently higher values than the DWD analyses. The systematic differences between both data sets are probably not only due to different methods in the analyses schemes but also to differences in the availability of observational data. For the NMC analyses in addition to the operational data distributed in the GTS, experimental NIMBUS 6 soundings and experimental cloud track winds derived at the University of Wisconsin were also used. As the

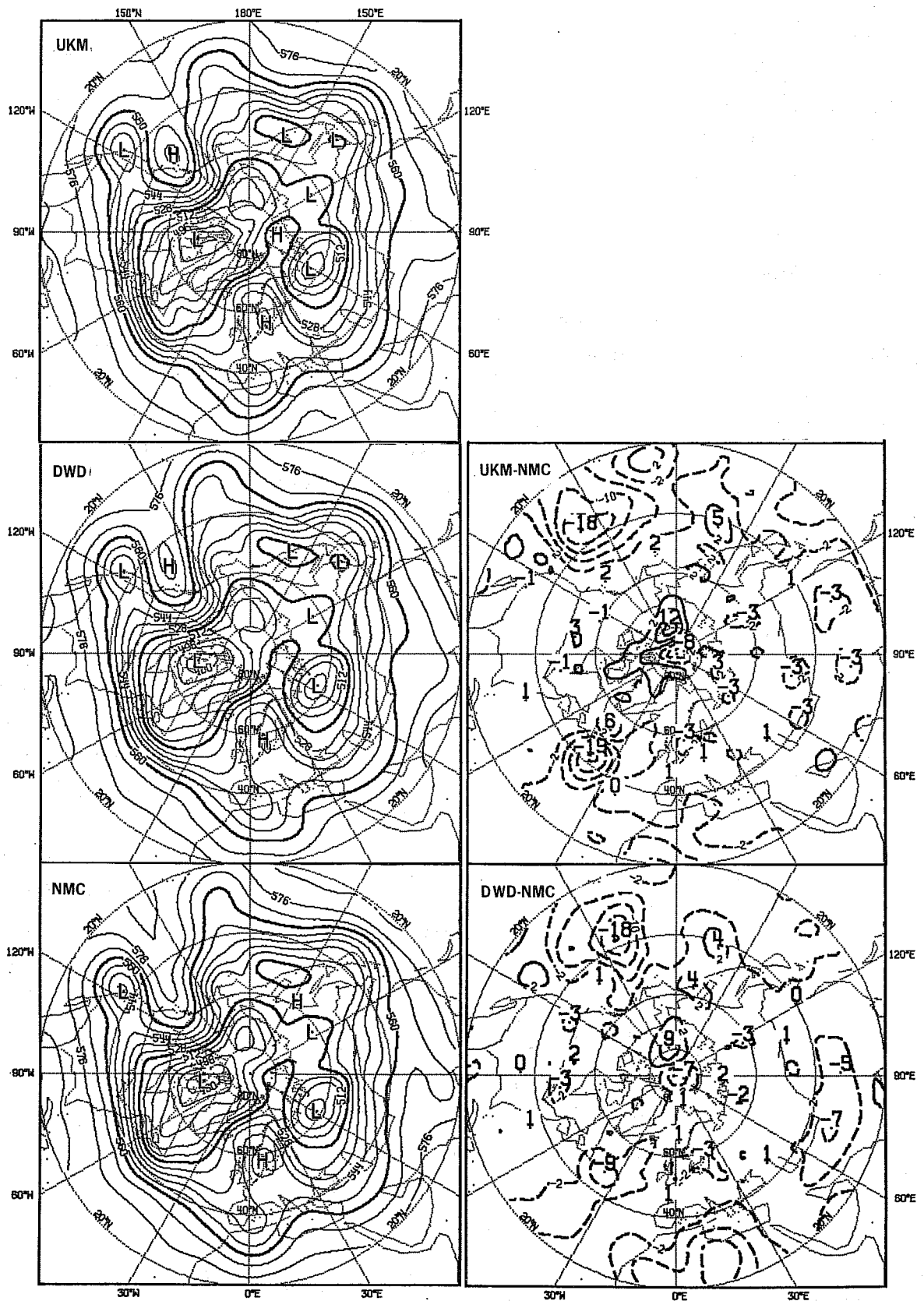


Fig. 1 Left: Analyses of the 500 mb height field by the meteorological Centres in the US (NMC), in Germany (DWD) and in the United Kingdom (UKM) for the 6th February 1976.
 Right: Difference maps UKM-NMC and DWD-NMC.

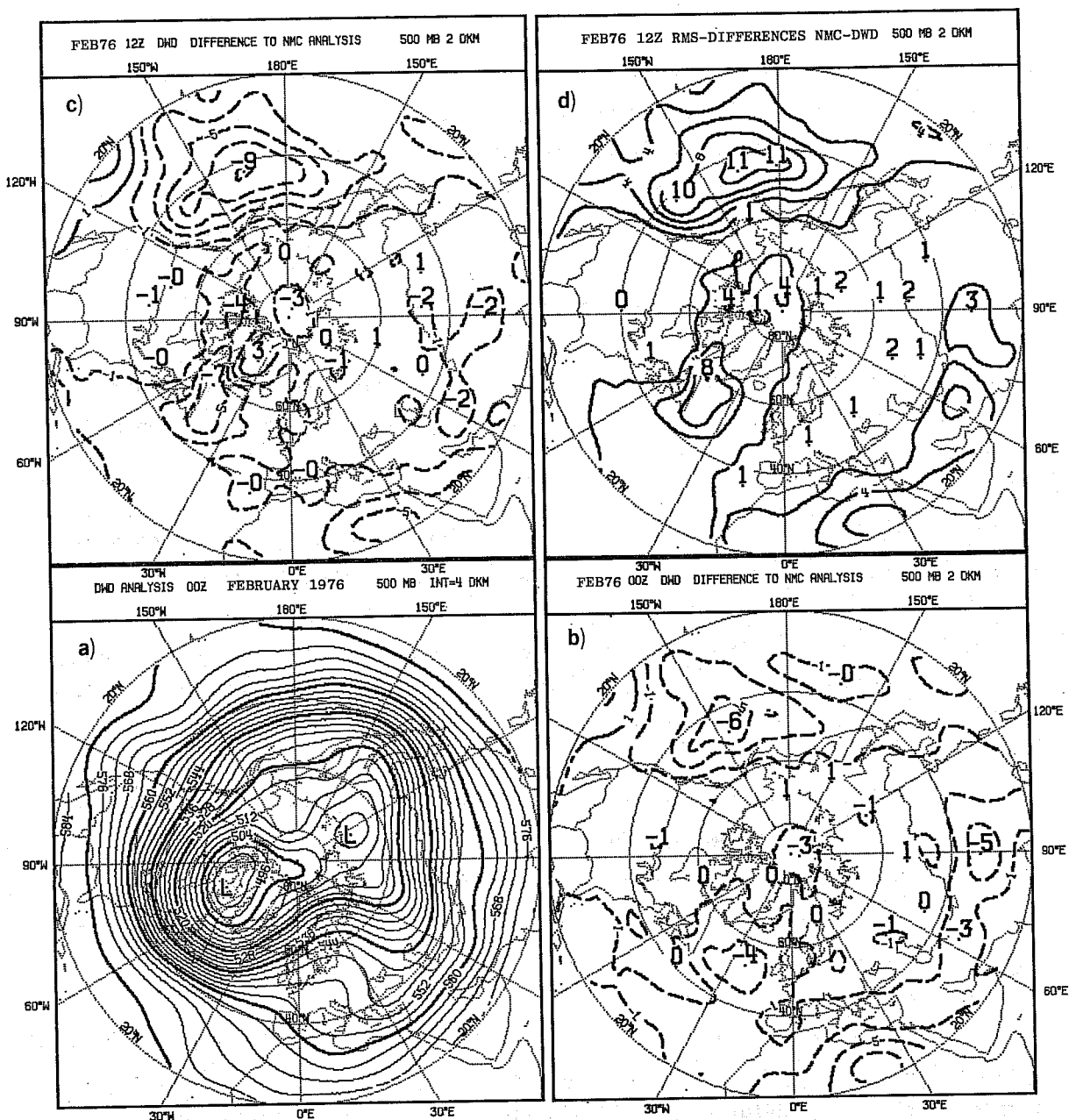


Fig. 2 Mean 500 mb height field for the period 3 to 27 February 1976.

- a) DWD analyses at 00Z
- b) Mean differences of 00Z analyses DWD-NMC
- c) Mean differences of 12Z analyses DWD-NMC
- d) Rms differences of 12Z analyses DWD-NMC

pattern in the difference maps is similar to those obtained in experiments comparing analyses with and without use of satellite temperature soundings (Desmarais et al, 1978) the differences between both analyses may partly be due to the different use of satellite data. This would be supported by the fact that 12Z analyses have larger differences over the Pacific because there are less surface based observations at night-time available which will give even higher influence of satellite data on the NMC analyses.

We will not go further into the reasons for the differences, but concentrate on making the differences obvious and showing their impact on verification and diagnostics.

In Fig.2 a map of rms-differences between NMC and DWD analyses are also shown (panel d). The similarity between panels b and d, which both compare the 12Z analyses, is quite strong. It means that the rms differences are dominated by the mean error field. The daily variations adding only 10 to 20 m over most areas. Nevertheless, the rms differences of the transient part alone can be as large as 63 m, e.g. over the Pacific.

In Fig. 3 variations with time (1 to 11 February 1976) and with height of the rms differences between DWD and NMC are shown. Area means between 20°N and 82.5°N of the total rms differences and contributions by zonal means and two wavenumber groups are displayed separately. (For the definition of verification scores, see Appendix).

The rms differences can also be separated into contributions by area (meridional) means and by their deviations. The latter one is the standard deviation. When comparing standard deviations and rms differences, it becomes obvious that more than half of the rms differences of zonal means are due to their meridional means, e.g. on day $7\frac{1}{2}$ at 300 mb we find rms differences of 25 m, the standard deviation is 16 m and the rms difference of the area mean follows then to be 19 m.

The total rms differences as well as the contributions by wavenumber groups show highest values at the upper troposphere where variances of the height fields are largest and decrease to lower levels.

A further insight into the differences can be obtained from anomaly correlation coefficients which give mainly information about differences in positions of troughs and ridges. For the definition of the anomaly correlation and other skill scores, see Appendix. Fig. 4 shows height-time cross sections of area means between 20°N and 82.5°N of anomaly correlation coefficients. Overall we find rather high coefficients mostly higher than 96%. That means that the

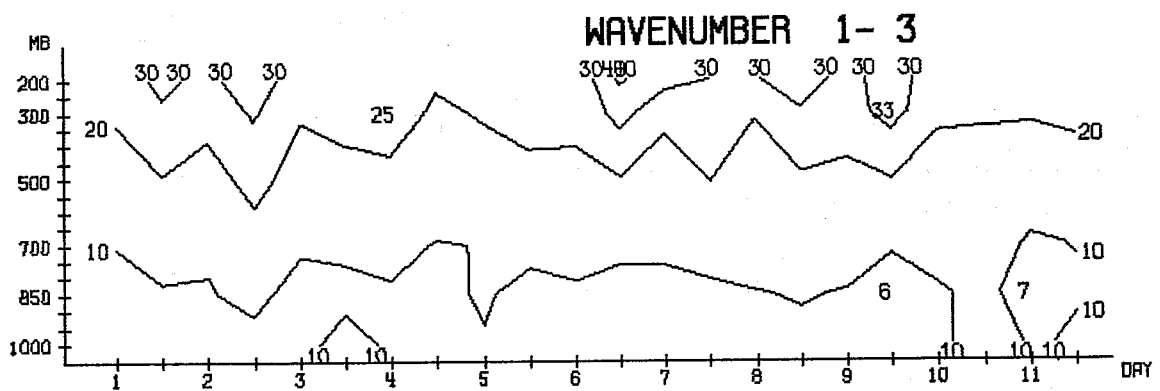
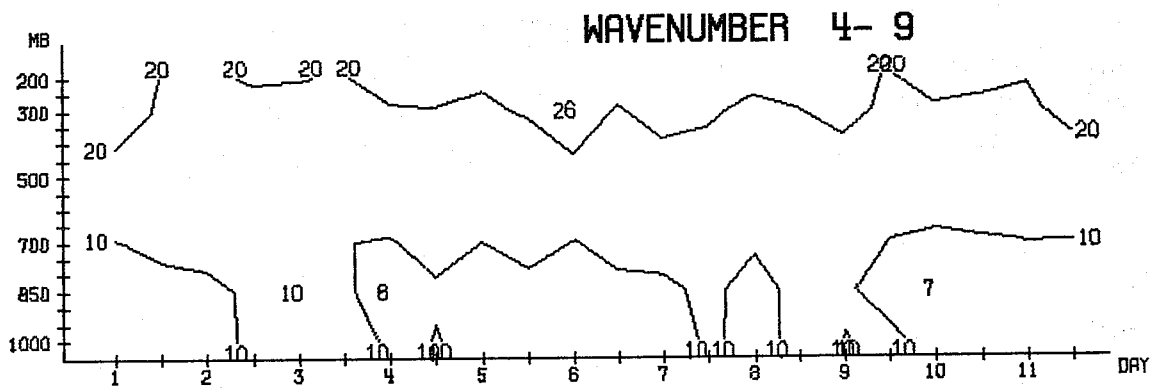
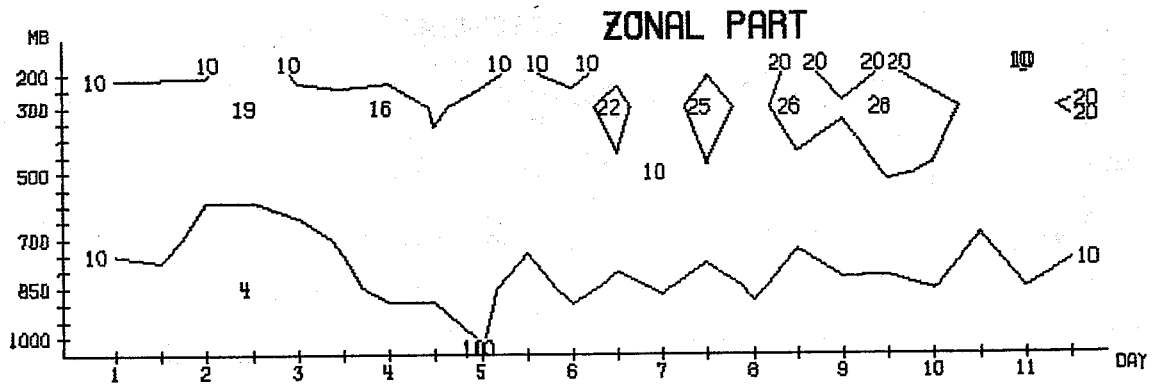
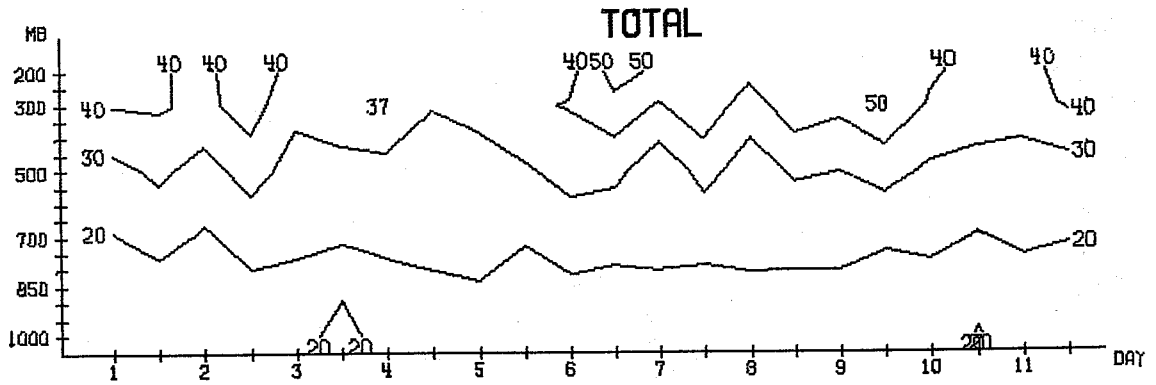


Fig. 3 Variability with time and pressure of the rms-differences of height fields (m) between NMC and DWD analyses. Period from 1 to 11 February 1976. Mean between 20 and 82.5°N.

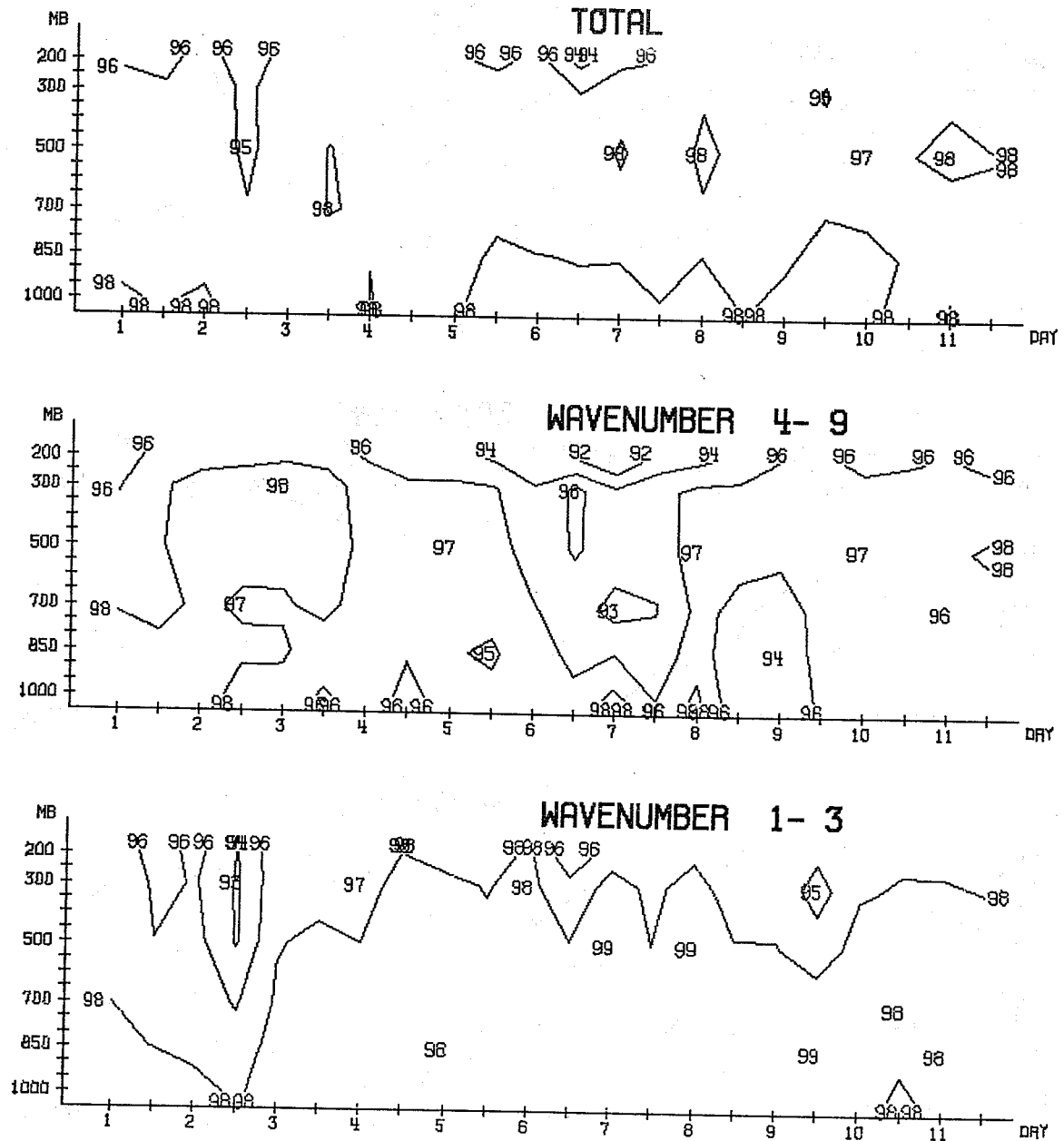


Fig. 4 Variability with time and pressure of the anomaly correlation coefficients of height fields (%) between NMC and DWD analyses. Period from 1 to 11 February 1976. Mean between 20 and 82.5°N.

rms differences we found earlier, are mainly due to differences in the intensity of troughs and ridges but not in their positions. There are a few days which show stronger deviations in the positions, e.g. on day 2½ at the long waves and about day 7 at the medium waves. Noteworthy are also lower correlation coefficients at 1000 mb for the medium waves (4 - 9).

Fig. 5 shows the rms differences of the temperature between NMC and DWD analyses. We have left out the 1000 mb level because it is the most difficult level to analyse, due to local effects. A noticeable vertical structure for the whole period can be found. The values at 500 mb are almost half of those at 850 mb

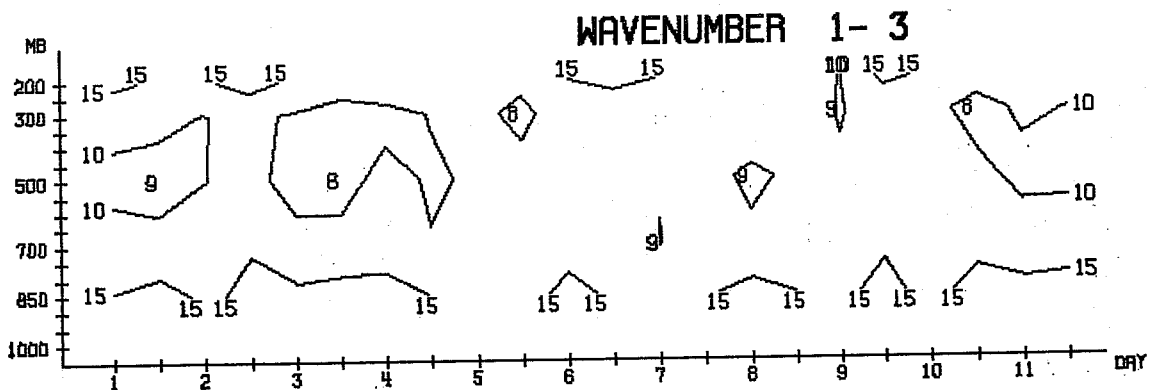
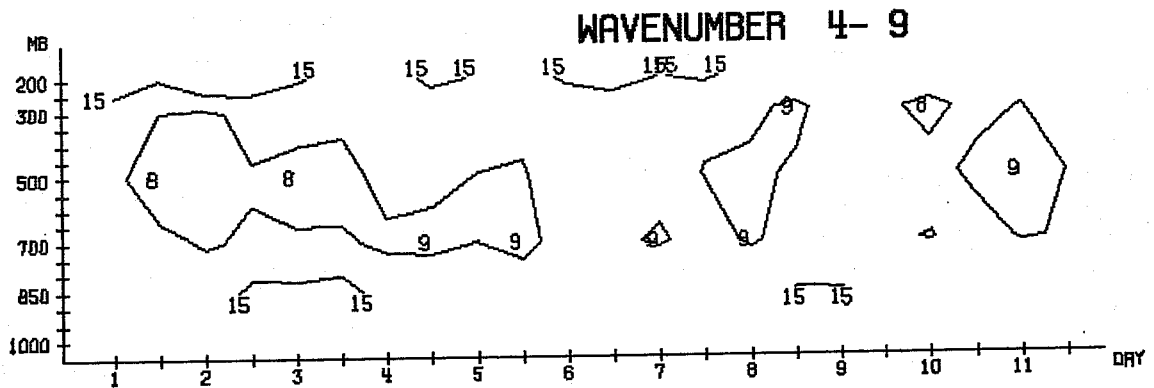
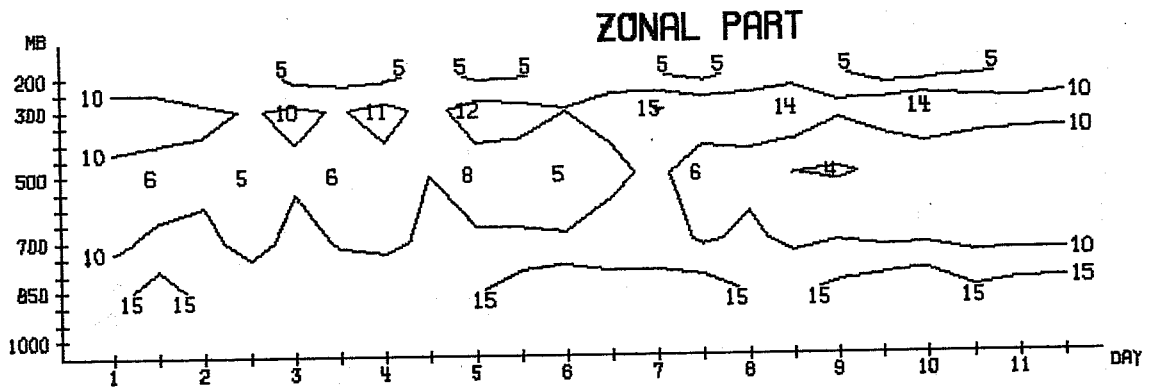
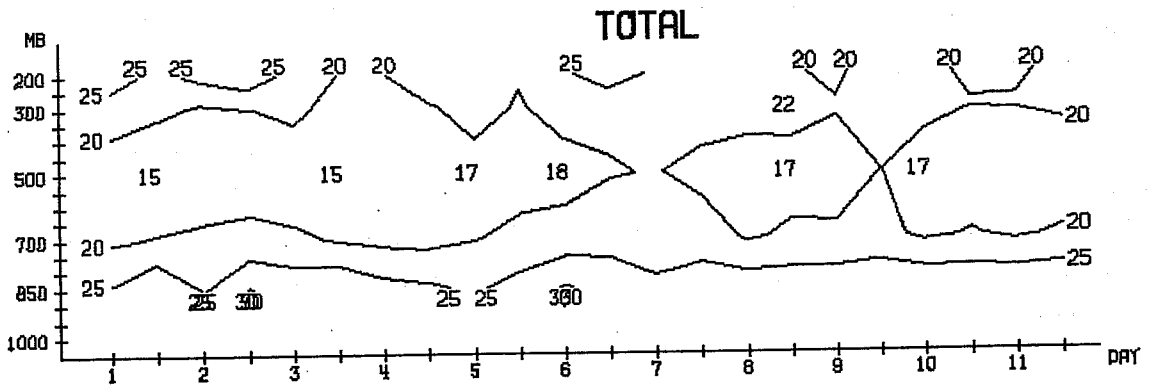


Fig. 5 Variability with time and pressure of the rms-differences of temperature fields ($\frac{1}{10}^{\circ}\text{C}$) between NMC and DWD analyses. Period from 1 to 11 February 1976. Mean between 20 and 82.5 $^{\circ}\text{N}$.

and 200 mb. In the zonal part there is even an increase from 0.5°C at 500 mb to more than 1.5°C at 850 mb.

With Figs. 6 and 7 a deeper insight into the zonal means and their meridional variations shall be gained. This time a mean over the whole month of February 1976 has been taken. At 1000 mb (Fig. 6) it is remarkable that the mean subtropical height ridge is analysed 5° further north and somewhat less intense by DWD than by NMC.

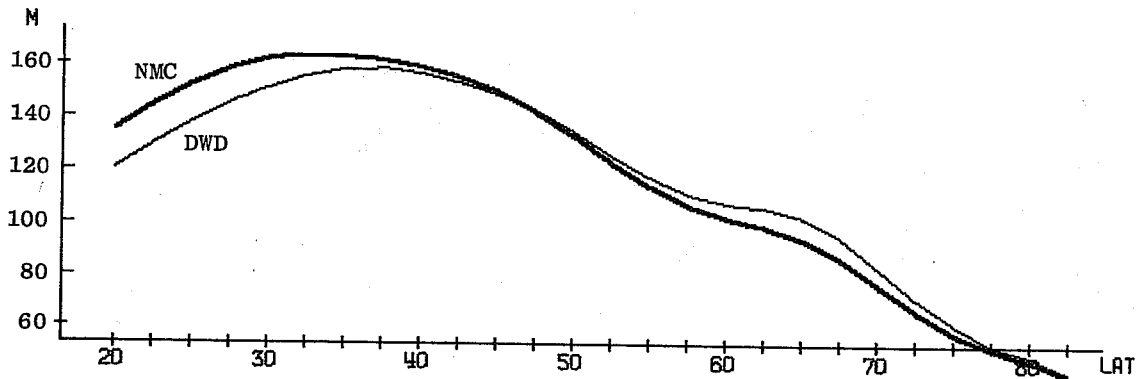


Fig. 6 Zonal mean of 1000 mb height. Average for February 1976.

Fig. 7 gives an overview of the meridional and vertical variability of the temperature differences. Temperatures in the NMC analyses are lower than the DWD ones north of 45°N in the lower troposphere and south of 35°N in the middle troposphere, while opposite signs can be found in the upper troposphere north of 45°N and at 850 mb south of 40°N . These differences will have an effect on the vertical lapse rate of temperature by more than 3°C between 850 mb and 300 mb at polar latitudes and a little less at 20°N with the opposite sign. It also results in differences in the meridional gradients of temperature. At 850 mb they are markedly smaller in the DWD analyses than in the NMC analyses, more than 3 K between 30°N and 65°N which is more than 10% of the gradient. At higher levels

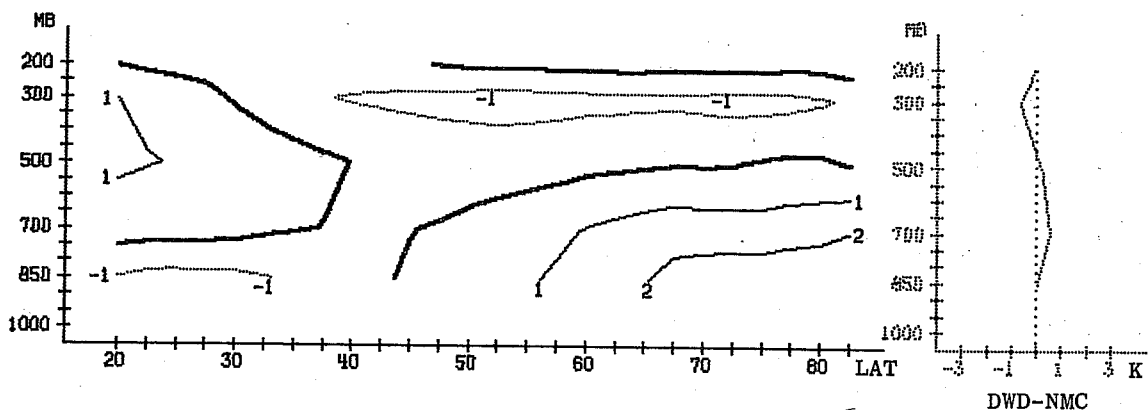


Fig. 7 Variability with pressure and latitude of zonal means of temperature. Averages for February 1976.

the differences are smaller and at 500 mb and 300 mb of reversed sign. The impact of this on diagnostic and verification parameters will be seen in the next section.

3. SENSITIVITY OF VERIFICATION AND DIAGNOSTIC PARAMETERS

The data sets used here to show the sensitivity of the parameters are, on the one hand, the two or three analysis sets mentioned earlier and on the other hand two sets of forecast experiments based on seven initial dates in February 1976. Both models for the forecast experiments differ only in their subgrid scale parameterization, one developed by GFDL (Smagorinsky, 1965, Miyakoda et al 1972) and the other by ECMWF (Tiedtke et al 1979). A full documentation of these experiments can be found in Hollingsworth et al (1979).

We will deal here only with those parameters where a different choice of verifying analyses would lead to different conclusions. Diagnostic parameters like energetics will be treated like verification scores because it has become common practice to use diagnostic parameters for verification purposes too. This is needed because the present skill of modelling has gained such a high level that it is becoming increasingly difficult to find a clear cut advantage of one model over another.

It should also be mentioned here that the initial data for the forecasts were taken from NMC, but due to interpolation to sigma levels, initialization and interpolation back to pressure levels the initial data of the forecast (day 0 in the diagrams) are quite different from NMC analyses and sometimes even closer to DWD analyses.

3.1 Rms-differences or standard deviations

In Section 2 we saw that rms-differences of the 500 mb height fields between two analyses ranged between 20 to 30 m. Rms-errors or standard deviations between analyses and forecasts are reaching values of 120 m after about 6 days. One would expect that choosing different analyses might change the rms errors. In the two experiment series used here, no remarkable difference could be spotted in the standard deviations of the height fields and are therefore not shown here. An impact can be expected in the rms errors of the zonal means due to different area mean heights of upper pressure levels. This is connected with different zonal mean temperatures and will be discussed in the section concerning the mean static stability. In the standard deviation of the temperature fields, however, a noticeable and important impact from the choice of analyses could be found. As the impact became even clearer in the correlation coefficients we will discuss it there (see Fig. 8).

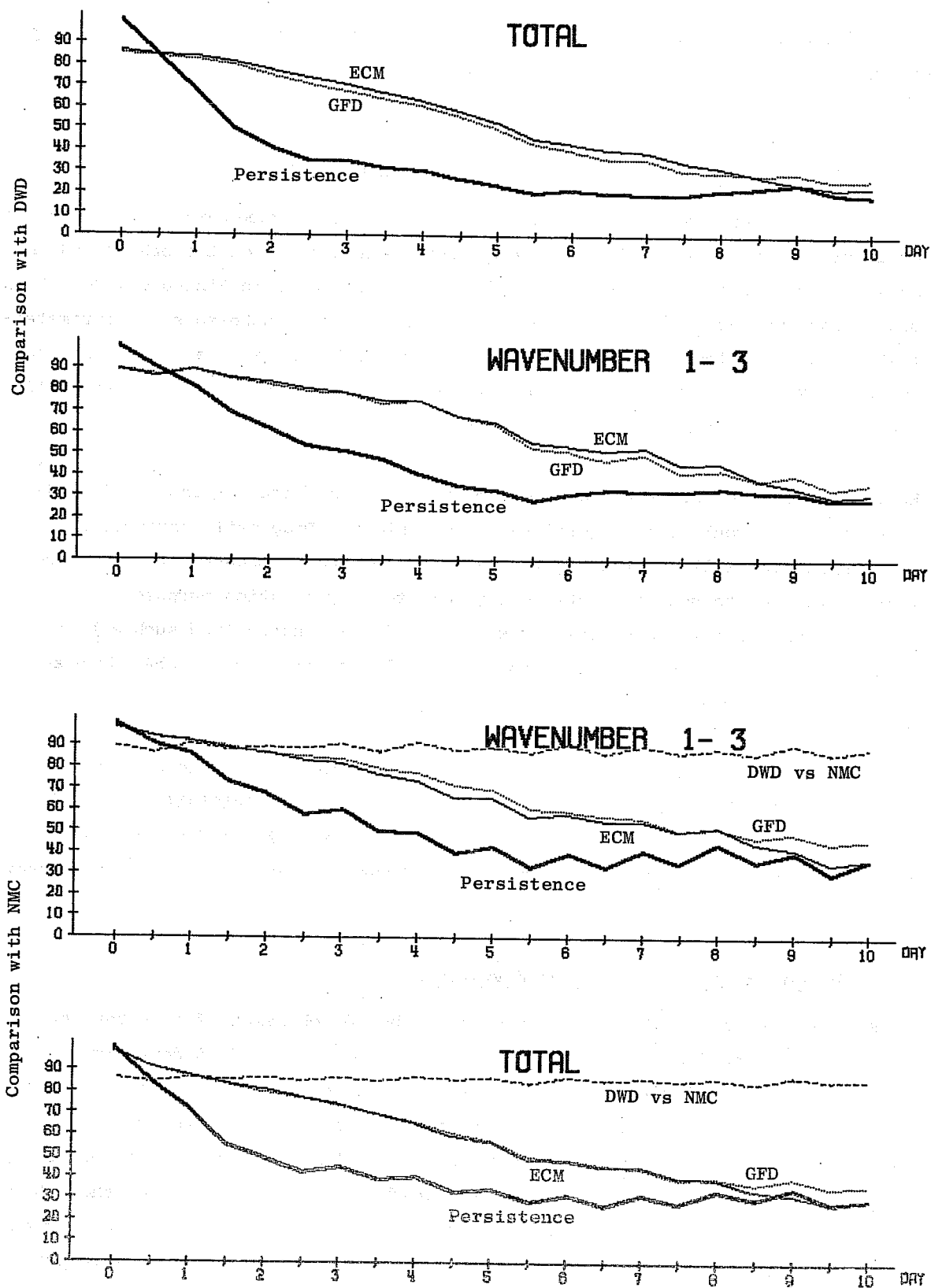


Fig. 8 Anomaly correlation coefficients of temperature (%) at the 850 mb level. Average between 20° and 82.5° N. Top panels: comparisons of forecasts with DWD analyses, lower panels: comparisons of forecasts with NMC analyses. Ensemble mean of 7 February 1976 cases. Heavy solid line: persistence forecast, thin solid line: ECM-forecasts, dotted line: GFD-forecasts, dashed line: DWD-NMC comparison.

3.2 Anomaly correlation coefficients

The anomaly correlation coefficients of the height fields between both analyses were quite high, mostly higher than 96% and, therefore, we would expect no impact on this skill score from the choice of the analyses.

The impact on the anomaly correlation coefficients of the 850 mb temperature fields can be seen in Fig. 8. Means of 7 cases of both experiment series are given. Both top panels show a comparison with DWD analyses for the total field and the contribution by the long waves. The lower panels show the corresponding values for a comparison with NMC analyses. A comparison between both analyses is also indicated by a dashed line, which lies between 85 and 90%.

A much stronger diurnal oscillation in the analyses by NMC than by DWD is indicated by the DWD-NMC comparison in combination with the heavy solid lines showing the skill of a persistence forecast. It is most obvious in the contributions by the long waves. The most important point here is the fact that the DWD analyses give a better score to the ECM-forecast, while the NMC analyses favour the GFD-forecast, especially at the long waves. Both forecasts arrive at higher correlation coefficients when using NMC analyses instead of DWD analyses, but the differences are strongest with the GFD-forecast. It must be admitted that a sample of 7 cases is quite small and that, therefore, the differences may be insignificant.

3.3 Static stability

We have seen before that the differences in the zonal mean temperatures between both analyses are quite large and show distinct vertical and meridional structures, which must have quite a strong influence on the mean static stability of the atmosphere.

Both panels in the middle of Fig. 9 show cross-sections of the static stability of both forecast experiments and the corresponding values of the analyses are in the top and bottom panel.

The vertical structure north of 50°N is similar in all panels with a minimum stability for the layer 500 to 700 mb, but the values differ considerably. We find that the ECM-model's results are quite close to those of the DWD analyses, showing a less stable atmosphere, while the GFD model agrees better with the NMC analyses with a more stable atmosphere.

The vertical structure between both analyses and between analyses and forecasts south of 40°N are quite different. The NMC analyses show lowest stability at

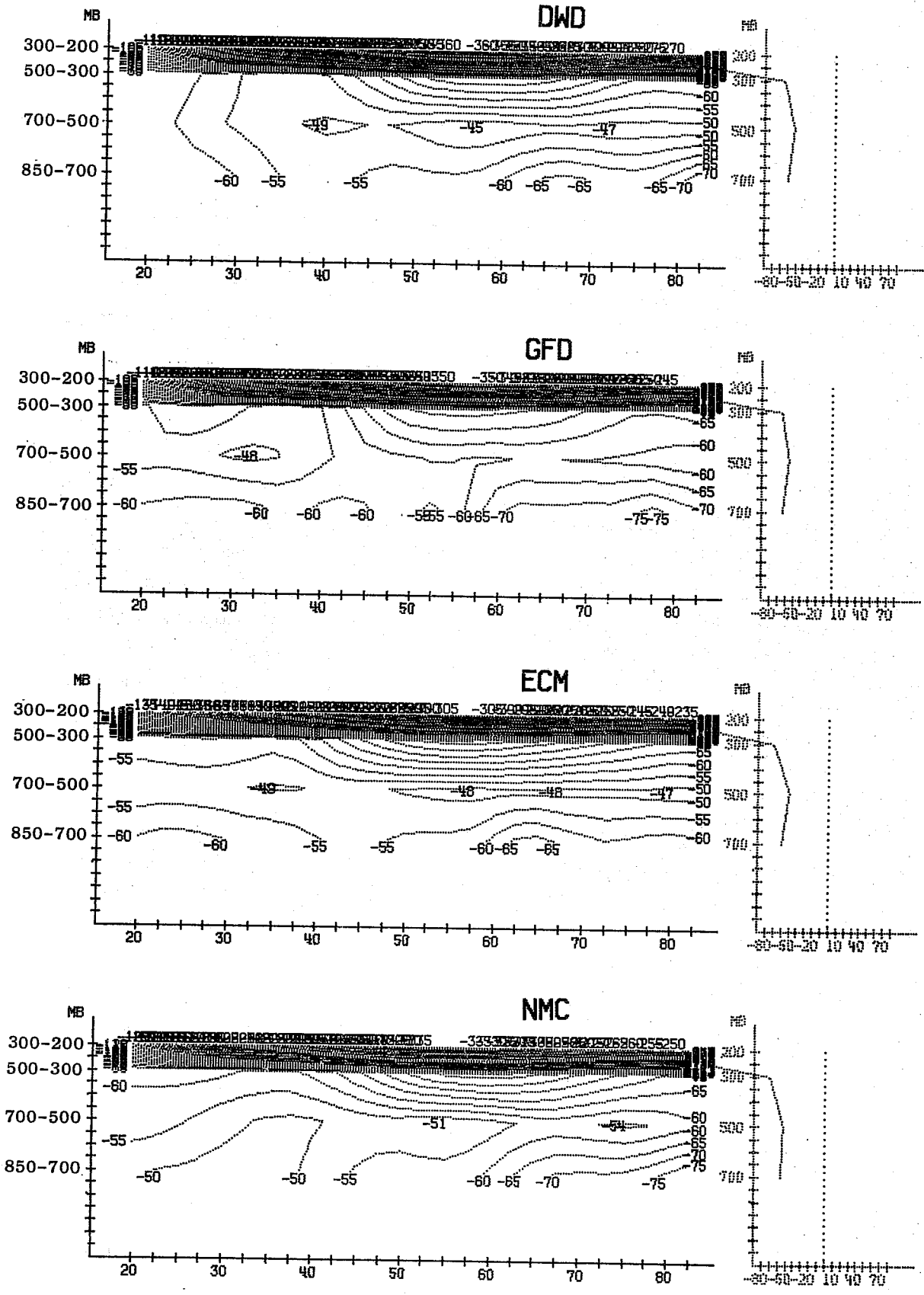


Fig. 9 Ensemble mean of static stability $\frac{\partial \theta}{\partial p}$ (K/bar) for two forecast experiment series (GFD and ECM) and for two corresponding analyses (DWD and NMC) during the last three days of ten day forecasts.

the lowest level; the DWD analyses have almost no structure, only a slight minimum for the layer 500 to 700 mb, while the forecast models have strong structures with minimum values at the same levels as DWD. Which of these structures is right.

As these differences in the values can easily be 20%, they must have a strong impact on all calculations concerning the available potential energy.

3.4 Available potential energy

In Fig. 10 we see an ensemble mean of the eddy available potential energy for both analyses and both forecast experiments. Again 7 cases have been averaged. If a greater ensemble would have been used, almost no time variation in the analyses should be seen but just a climatological mean for February. The values would show how far the model's climate differs from the real climate after the respective forecast time. This stage has obviously not been reached with 7 cases. Averages for the troposphere (850 - 200 mb) north of 20°N of contributions by two wavenumber groups, 1-3 and 4-9, are shown. Both analyses give fairly similar values for the long waves and also the forecast's values are quite close, except at the end of the forecast period. Differences become obvious at the medium waves (4-9). As may be expected from the differences in the static stability, DWD analyses and ECM forecasts have higher values than

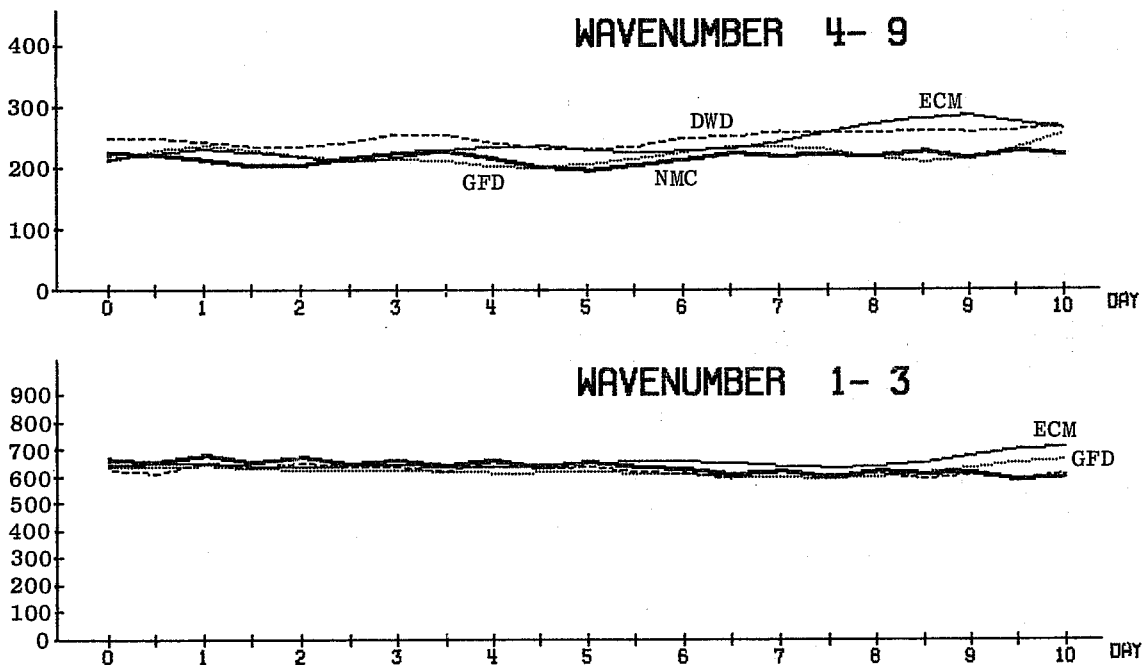


Fig. 10 Ensemble mean of eddy available potential energy (kJ/m^2) separated in wavenumber groups for two forecast experiment series (GFD and ECM) and two corresponding analyses (DWD and NMC). Integral between 850 mb and 200 mb, average between 20°N and 82.5°N.

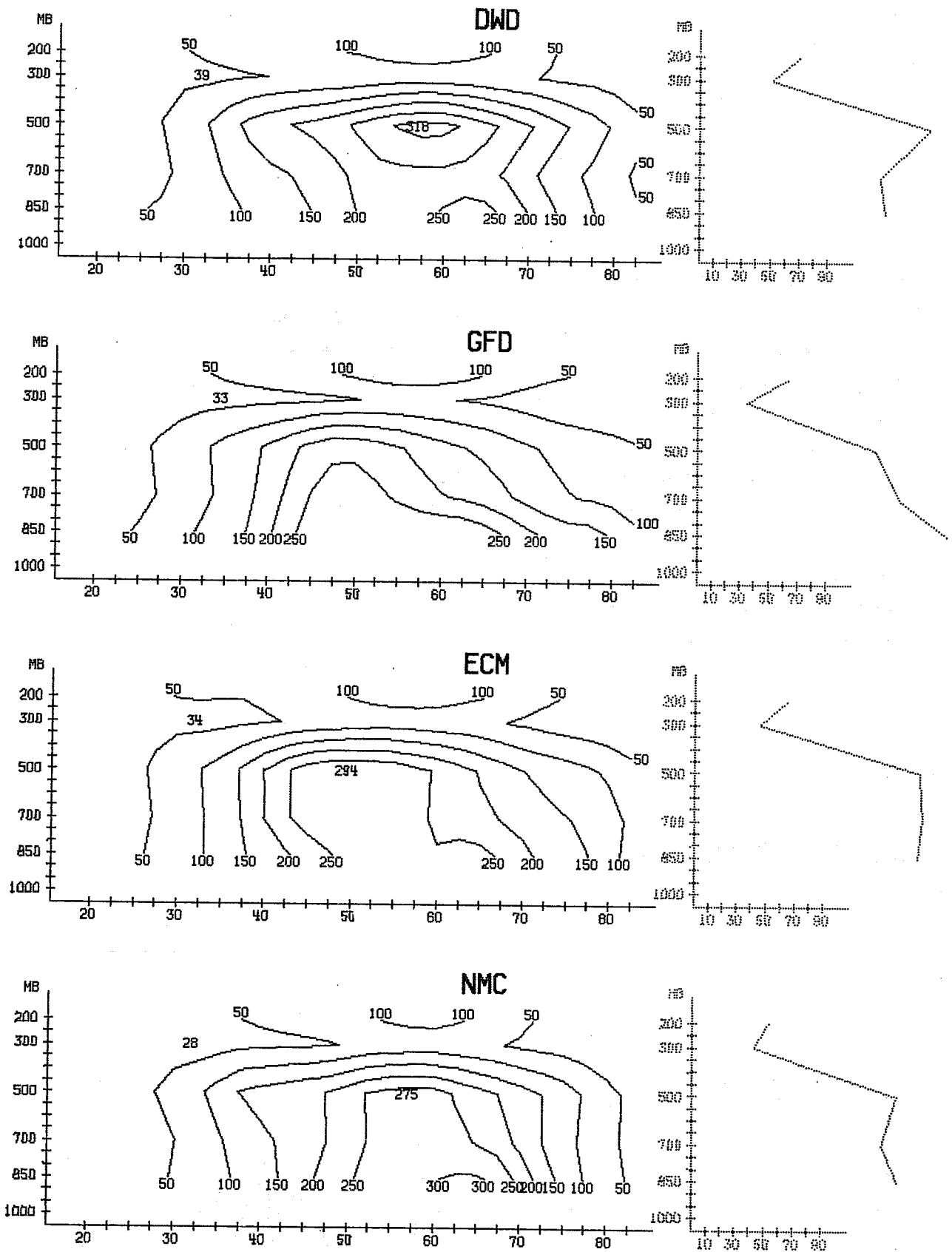


Fig. 11 Latitude-pressure cross-section of eddy available potential energy (10 kJ/m^2) for the 7th to 10th day of forecast, comparing two forecast experiment series (GFD and ECM) with the corresponding values of two difference analyses (DWD and NMC)

NMC analyses and GFD forecasts. Again, the choice of verifying analyses is very important for the evaluation of the forecasts.

We should also expect similar differences for the long waves, because of the static stability. As this is not found, it can be concluded that the higher static stability in the NMC analyses and GFD-forecasts is compensated by higher variances in the temperature fields in the long waves.

To find out the real deficiencies of the forecast, we have to go into more detail. Fig. 11 shows height-latitude cross-sections of the eddy available potential energy averaged over the last three days of the forecast period for the 7 cases mentioned before. Here we see that it is not so much the amount of available potential energy that the forecasts differ from observations, but in its distribution. The GFD forecast is wrong in the vertical structure and both forecasts have the position of the maximum too far south.

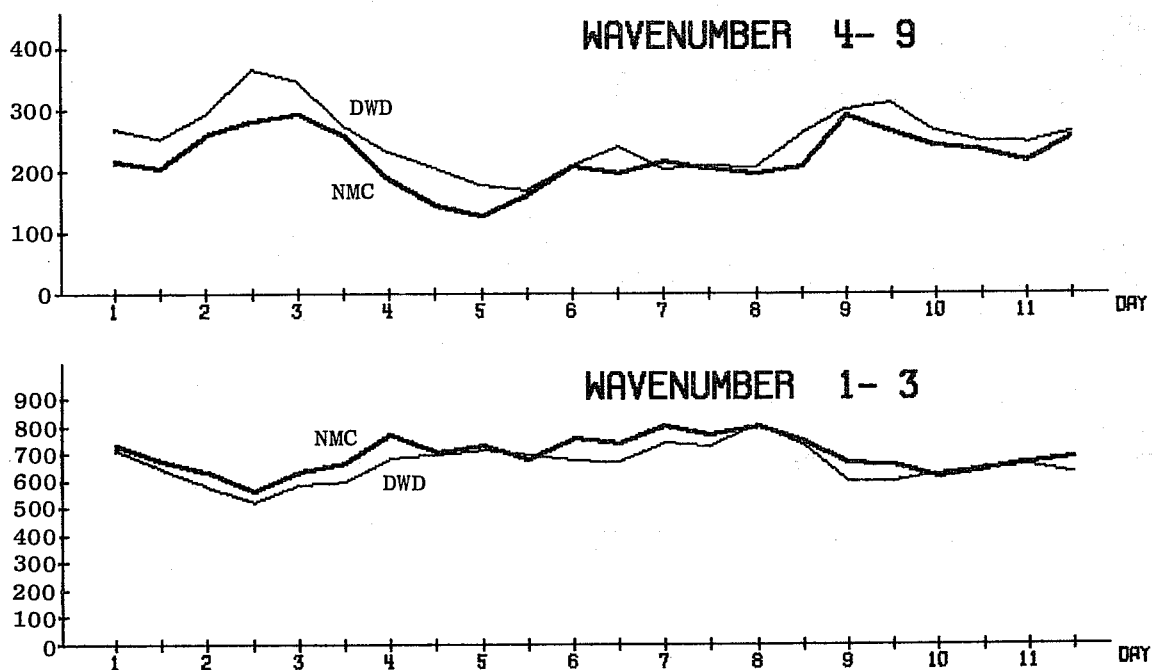


Fig. 12 Time sequence of available potential energy (kJ/m^2) for two analyses sets. Integrated from 850 to 200 mb and averaged between 20°N and 82.5°N .

For diagnostic studies it is sometimes less important to be concerned with the level of energy than to find sequences of extreme. In Fig. 12 such a time sequence from the first to the 11 February 1976 can be found for both analyses. There are a few dates when minima or maxima fall on times which differ between half a day to one day, e.g. the 3rd, 5th and 9th February 1976 at the medium waves. At the long waves even different courses can be found between the 4th and 6th February 1976 with a slight relative maximum in the DWD data, while the

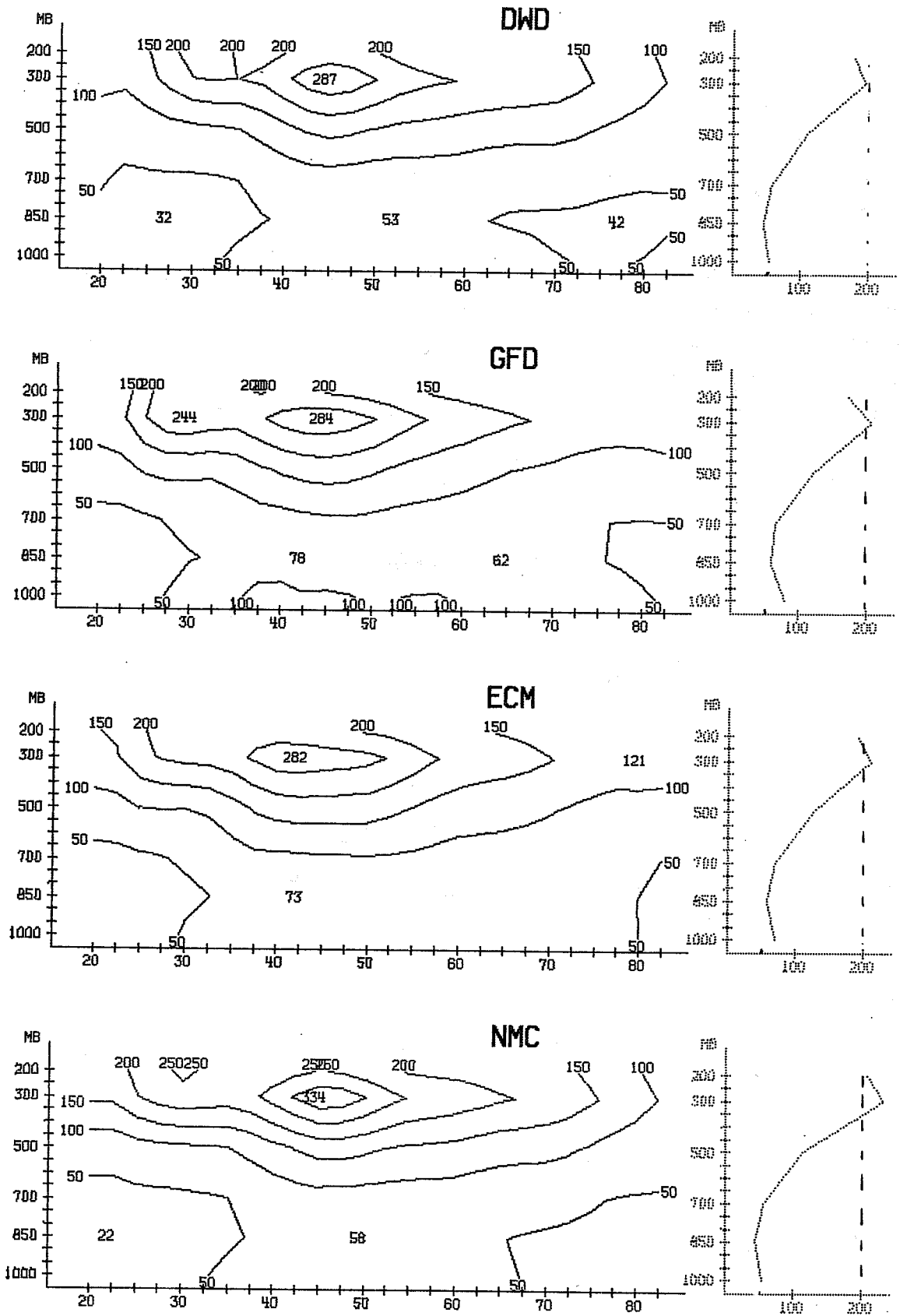


Fig. 13 Same as Fig. 11 for geostrophic eddy kinetic energy.
Units $10 \text{ kJ m}^{-2} \text{ bar}^{-1}$

NMC show a minimum.

3.5 Kinetic energy

In Fig.13 we see a pressure-latitude cross-section of eddy kinetic energy of both analyses and of both forecasts, it is the same mean of 7 cases averaged for the last 3 days of 10 day forecasts as before. For an easier comparison geostrophic winds have been used. We find a relative maximum at 45°N at 300 mb, which is probably connected with the polar jet. The maximum values are $3340 \text{ kJ m}^{-2} \text{ bar}^{-1}$ for the NMC analyses on the one hand and about $2840 \text{ kJ m}^{-2} \text{ bar}^{-1}$ for the DWD analyses or the forecasts on the other hand. A second maximum at 30°N and 200 mb shows again considerable differences in its values between both analyses. In the GFD forecast this maximum has a value near to that of the NMC analyses, but at too low a level, while the ECM value is nearer to the DWD solution. On the whole the structure in all panels is quite similar. The areal averages for each level, shown in the diagram on the right, make it clear that the eddy kinetic energy of the models lies just between those of the analyses in the upper troposphere while it is too high compared with both analyses in the lower troposphere.

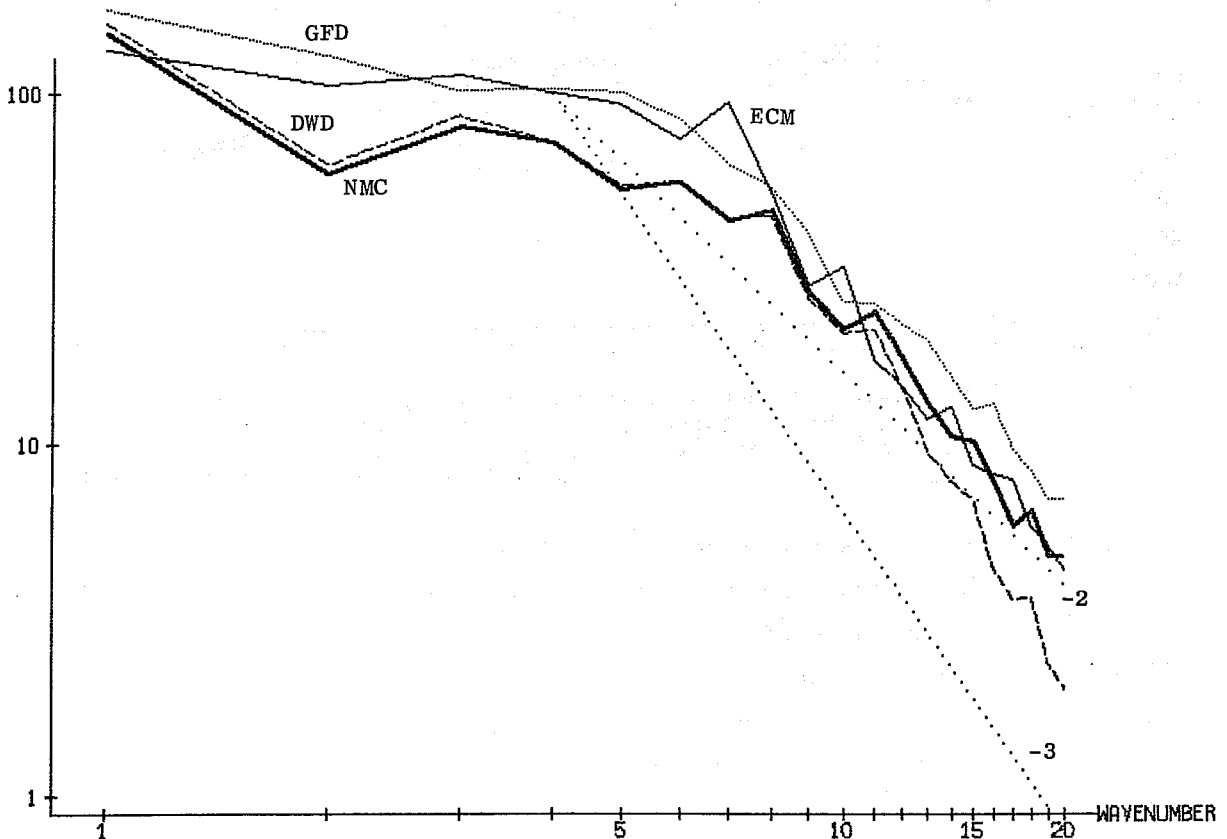


Fig. 14 Spectra of geostrophic kinetic energy ($\text{kJ m}^{-2} \text{ bar}^{-1}$) for the 7th to 10th day forecast, comparing two forecast experiment series (ECM and GFD) with the corresponding analyses (DWD, and NMC). Average between 40° and 60°N , 1000 mb level.

Fig. 14 shows the spectrum of the geostrophic kinetic energy for the 1000 mb level, where the forecasts were quite different from the analyses. It should be stressed here that the panels on the right of Fig. 13 were an average between 20°N and 82.5°N , while Fig. 14 is an average between 40°N and 60°N . The latter latitudinal belt was chosen smaller than the other one to avoid mixing of waves with too large differences in actual lengths.

It is obvious that the differences between analyses and forecasts are due to contributions by the long waves with wavenumbers 2 to 7, while at higher wavenumbers the differences between both analyses are as large as the differences between analyses and forecasts.

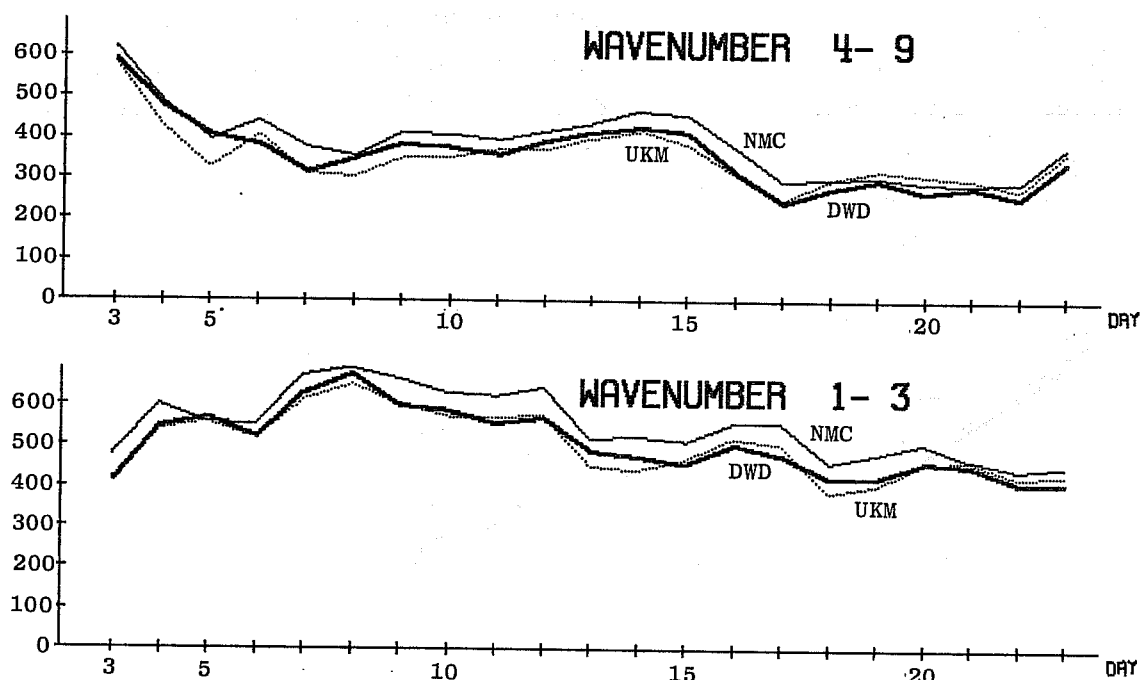


Fig. 15 Time sequence of geostrophic kinetic energy (kJ m^{-2}) for three sets of analyses. Integrated from 1000 to 200 mb and averaged between 20°N and 82.5°N . Period 3 to 23 February 1976.

In Fig. 15 we want to see a time sequence of kinetic energy to find out if diagnostic studies mainly concerned with occurrences of special events, such as special peaks, are affected by the choice of analyses schemes. This time the UKM analyses are also included. As in Fig. 12 showing the available potential energy we find that the occurrence of peaks may be shifted by one day. Differences in the shape can also be found, see, e.g. wavenumber 4-9 on Day 5.

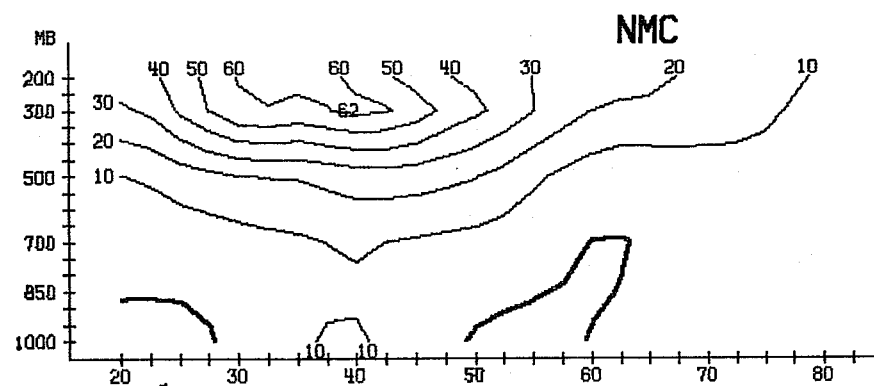
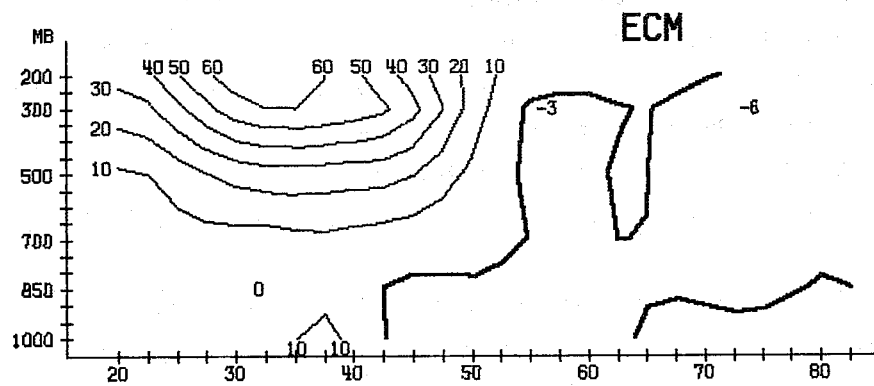
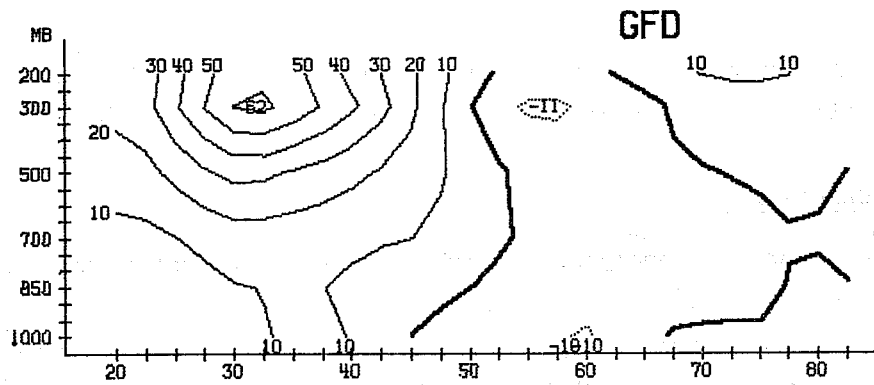
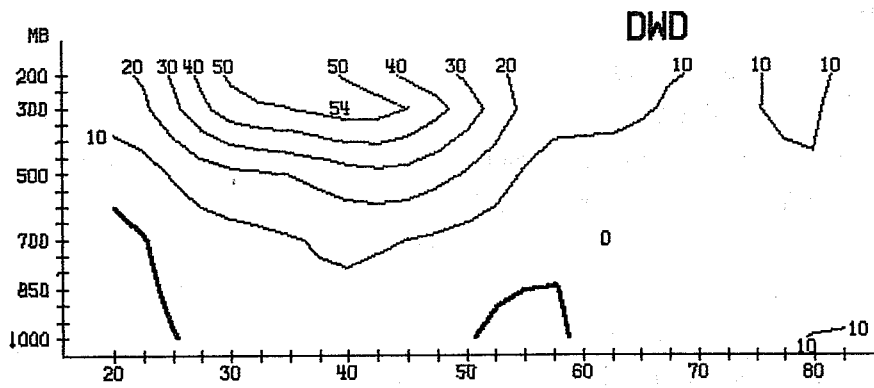


Fig. 16 Same as Fig. 11 for geostrophic eddy momentum flux.
Units $m^2 s^{-2}$.

3.6 Momentum flux uv

Another important diagnostic parameter is the momentum-flux. Fig. 16 shows the geostrophic eddy momentum flux for both analysis schemes and both forecast series. If we look at the area south of 45°N quite a good similarity between all 4 panels can be found. The results by the DWD deviate most, and the values are about $10 \text{ m}^2 \text{ s}^{-2}$ less than those of the NMC analyses or the forecasts.

North of 45°N all panels look different. The NMC analyses still keep rather high positive numbers, while the models tend to negative values. The DWD analyses lie just between both extremes.

As this parameter goes into the calculation of the transfer between eddy and zonal kinetic energy, we might expect similar difficulties there too.

4. CONCLUSIONS

It has been shown that analyses by different meteorological centres may differ in many respects. Differences in the 500 mb height fields can be larger than 200 m in data sparse areas, e.g. over the Pacific. Part of the large differences are systematic due to different selection or weighting of data or to the analysing method. The maximum systematic difference of the 500 mb height field was 90 m. The differences in the height fields are connected with differences in the temperature fields and are even more obvious there. In February 1976 the zonal means of 850 mb temperatures analysed by NMC are up to 3 K apart from those by DWD. The impact of these differences can be as much as 20% in the static stability and 10% in the mean meridional temperature gradient.

Differences in the very large scaled longitudinal distribution of the 850 mb temperature fields lead to an advantage of one forecast experiment series against another one of 5% in the anomaly correlation coefficients when comparing the forecasts with NMC analyses which vanished or even reversed when using DWD analyses.

It cannot yet be judged which of both analyses schemes is right or better and investigations should be continued. The present investigation should be a warning when verification or diagnostic studies are carried out, especially when using temperature or derivatives of the height fields.

REFERENCES

- Bliesner, B.O., Baumhefner, D.P., Schlatter, T.W. and Bleck, R. 1977 A comparison of several meteorological analysis schemes over a data-rich region. Mon.Wea.Rev., 105, 1083-1091.
- Crutcher, H.L. and Jenne, R.J. 1970 "An interim note on northern hemisphere climatological grid data tape", NOAA Environmental Data Service, NWRC, Ashville
- Desmarais, A., Tracton, S., McPherson, R. and Van Haaren, R. 1978 The NMC Report on the Data System Test. National Meteorological Center, Camp Springs, Maryland, USA.
- Hollingsworth, A., Arpe, K., Tiedtke, M., Capaldo, M., Savijärvi, H., Åkesson, O. and Woods, J.A. 1979 Comparison of medium range forecasts made with two parameterisation schemes. ECMWF Technical Report No. 13, 206 p.
- Miyakoda, K., Hembree, G.D., Strickler, R.F. and Shulman, I. 1972 "Cumulative results for extended forecast experiments. I Model performance for Winter cases", Mon.Wea.Rev., 100, 836-855.
- Smagorinsky, J., Manabe, S. and Holloway, J.L. 1965 "Numerical results from a nine-level general circulation model of the atmosphere", Mon.Wea.Rev., 93, 727-768.
- Tiedtke, M., Geleyn, J.F., Hollingsworth, A. and Louis, J.F. 1979 "Parameterization of sub-grid Scale Processes" ECMWF Technical Report No. 10

APPENDIX - DEFINITION OF SCORES

As the measures for forecast skill are not yet uniform in the literature, one has to be careful when comparing the results of our experiments with those of other authors.

We used the following formulation for the calculations of standard deviations and anomaly correlation coefficients:

The error of a quantity X is given by

$$\delta X(t) = X_p(t) - X_o(t)$$

where $X_p(t)$ and $X_o(t)$ are the predicted and observe (analysed) values at the predicted time, t, respectively. If two sets of analyses are compared $X_p(t)$ is the second analyses set. The anomaly is defined by

$$\Delta X(t) = X(t) - X_n$$

where X_n is the climatological (normal) value for February. The climatological values were taken from Crutcher and Jenne (1970). We used two averaging operators, one for an area mean or vertical average:

$$\bar{X} = \frac{\sum_i g_i X_i}{\sum_i g_i}$$

where X_i is an arbitrary variable at the grid point i and g_i is a weighting factor. As we had a regular latitude-longitude grid we used the cosine of latitude as weighting factors. Vertical averages were, of course, weighted by pressure.

The second type of averaging is an ensemble mean for a sample of N forecast experiments or days of analyses.

$$E(X) = \frac{1}{N} \sum_{n=1}^N X_n$$

where X_n is the value of skill score for a particular case.

$$\begin{aligned} \text{rms difference} &= E \left\{ \sqrt{\delta X^2} \right\} \\ \text{standard deviation} &= E \left\{ \sqrt{(\delta X - \bar{\delta X})^2} \right\} \\ \text{persistence standard deviation} &= E \left\{ \sqrt{(X_o(t) - X_o(t_o) - [X_o(t) - X_o(t_o)])^2} \right\} \end{aligned}$$

$$\text{NORM} = \frac{1}{T} \sum_{t=1}^T \sqrt{(\Delta X_o(t) - \overline{\Delta X_o(t)})^2}$$

T means a period of 6 February months which were taken from the NMC operational analyses from 1965 to 1970.

$$\text{anomaly correlation} = E \left(\frac{(\Delta X_p(t) - \overline{\Delta X_p(t)}) (\Delta X_o(t) - \overline{\Delta X_o(t)})}{\sqrt{(\Delta X_p(t) - \overline{\Delta X_p(t)})^2} \cdot \sqrt{(\Delta X_o(t) - \overline{\Delta X_o(t)})^2}} \right)$$

$$\text{anomaly correlation of persistence} = E \left(\frac{(\Delta X_o(t_o) - \overline{\Delta X_o(t_o)}) (\Delta X_o(t) - \overline{\Delta X_o(t)})}{\sqrt{(\Delta X_o(t_o) - \overline{\Delta X_o(t_o)})^2} \cdot \sqrt{(\Delta X_o(t) - \overline{\Delta X_o(t)})^2}} \right)$$

To enable a separation into contributions by disturbances of different scales the calculations are based on Fourier-series. The transformation of the formulae given above into wavenumber domain is straightforward but not given here because they look quite complicated and would disguise the main points.

ECMWF PUBLISHED TECHNICAL REPORTS

- No.1 A Case Study of a Ten Day Prediction
- No.2 The Effect of Arithmetic Precisions on some Meteorological Integrations
- No.3 Mixed-Radix Fast Fourier Transforms without Reordering
- No.4 A Model for Medium-Range Weather Forecasting - Adiabatic Formulation
- No.5 A Study of some Parameterizations of Sub-Grid Processes in a Baroclinic Wave in a Two-Dimensional Model
- No.6 The ECMWF Analysis and Data Assimilation Scheme - Analysis of Mass and Wind Fields
- No.7 A Ten Day High Resolution Non-Adiabatic Spectral Integration: A Comparative Study
- No.8 On the Asymptotic Behaviour of simple Stochastic-Dynamic Systems
- No.9 On Balance Requirements as Initial Conditions
- No.10 ECMWF Model - Parameterization of Sub-Grid Processes
- No.11 Normal Mode Initialization for a multi-level Gridpoint Model
- No.12 Data Assimilation Experiments
- No.13 Comparison of Medium Range Forecasts made with two Parameterization Schemes
- No.14 On Initial Conditions for Non-Hydrostatic Models
- No.15 Adiabatic Formulation and Organization of ECMWF's Spectral Model
- No.16 Model Studies of a Developing Boundary Layer over the Ocean
- No.17 The Response of a Global Barotropic Model to Forcing by Large-Scale Orography
- No.18 Confidence Limits for Verification and Energetics Studies